Eur. Phys. J. D **4**, 73–81 (1998)

**THE EUROPEAN PHYSICAL JOURNAL D**



# Creation and manipulation of coherences in molecules with a pulsed magnetic field

H. Ring, R.T. Carter, and J.R. Huber[a]

Physikalisch-Chemisches Institut der Universität Zürich, Winterthurerstrasse 190, 8057 Zürich, Switzerland

Received: 8 April 1998 / Accepted: 3 June 1998

**Abstract.** We demonstrate the application of a pulsed magnetic field for the creation and manipulation of coherences in molecular systems, using quantum beat spectroscopy for the detection of the dynamics of the molecular superposition states. In all cases, the experiments are performed on energy levels in electronically excited states of the (jet-cooled) $CS_2$ molecule populated by a short laser pulse. In the basic experiment, following excitation of initially degenerate Zeeman sublevels under zero field conditions with suitable laser polarization, quantum beats are generated at the moment the magnetic field is switched on, even when the field is delayed by several excited state lifetimes. By quenching of the field, it is shown that the molecule may be "frozen" in any superposition state of the participating sublevels. Using a combination of static and pulsed fields with different orientations, the molecule can be prepared in a more general state, described by coherences among all Zeeman substrates. This is achieved by choosing an appropriate time delay for the switched field, without any change to the geometrical parameters of the experiment such as laser polarization or detection direction. Numerical simulations of these dynamical coherence phenomena have been performed to support assignment and interpretation of the experimental results.

**PACS.** 42.50.Md Optical transient phenomena: quantum beats, photon echo, free-induction decay, dephasings and revivals, optical nutation, and self-induced transparency – 33.55.Be Zeeman and Stark effects – 33.80.-b Photon interactions with molecules

## 1 Introduction

The preparation of coherences among molecular states and their manifestation as quantum beats in the emission decay can be utilized as a powerful spectroscopic tool [1–5]. This time-domain method is essentially Doppler-free and the resolution achievable is limited only by the lifetime of the coherently excited states. Its versatility for investigating the structure and dynamics of jet-cooled molecules [4,5], radicals [6] and small van der Waals complexes [7] has been demonstrated also in conjunction with double resonance and pump-probe techniques [8,9].

Control of coherences and control of coherent population transfer between specific quantum states in molecules has recently drawn attention in the literature [10]. Excitation schemes have been proposed and demonstrated particularly in the context of control of chemical reactions [11,12]. In the present study we are concerned with the creation and manipulation of coherences by a pulsed magnetic field with the aim of further exploring the properties of quantum beats in molecules. These results are an extension of our previous optical-radio-frequency study [13,14], where a pulsed or continuous radio-frequency field was applied to create coherences between molecular Zeeman levels and to transfer coherence between these levels.

[a] e-mail: jrhuber@pci.unizh.ch

The triatomic molecule $CS_2$, which has also been studied by high resolution Zeeman and hyperfine quantum beat spectroscopy [15,16] as well as by the above mentioned UV-rf double resonance method [13,14], was a good candidate for the coherence experiments. Laser excitation at $\sim 30\,000$ cm$^{-1}$ is used to prepare a single rotational level in either the $^3A_2$ state *via* the 17U system or in the $^1B_2$ state *via* the 6V system [17–20]. Both states possess lifetimes in the microsecond region which is most convenient for our purposes. In the basic experiment, the molecule is pumped by a 3 ns laser pulse to a rotational state $J = 1$ under zero field conditions. After a delay of one or several microseconds, the pulsed magnetic field is switched on, splitting the magnetic sublevels and creating Zeeman quantum beats.

## 2 Experimental

The main part of the apparatus has previously been described [3,13]. Briefly, UV radiation at 30 000–30 600 cm$^{-1}$ with Fourier limited bandwidth of 180 MHz and a pulse duration of 3 ns is generated by frequency doubling the output of a pulsed dye amplifier. The latter is pumped by an excimer laser and is seeded by a single mode ring laser (Coherent 699 Autoscan). In a vacuum chamber,

**Table 1.** Transitions in $CS_2$ used in the experiments, and the Lande $g$-factors and lifetimes of the prepared states.

| Band | Identification | $\tilde{\nu}$ [cm$^{-1}$] | $g_J$ | $\tau$ [$\mu$s] |
|---|---|---|---|---|
| 17R | $R(0)^a$ | 30 070.305 | 0.022 | 3.0 |
| 6V | $Q(2)^b$ | 30 529.1980 | 0.12 | 5.8 |

[a] Frequency measured in present work, $g_J$ and $\tau$ from reference [15].
[b] Data from reference [19].

the UV pulse is crossed 40 mm below the nozzle with a supersonic free molecular jet, generated by a pulsed piezoelectric valve. A mixture of 2.5% $CS_2$ in Ne or Ar at 1 bar is expanded through a 0.3 mm nozzle. In order to generate a magnetic field with a fast risetime, a pair of Helmholtz coils with a diameter of 55 mm and 7 windings per coil was placed around the crossing of laser and molecular beam. This set-up yields a magnetic field of up to ∼100 Gauss with a risetime of $< 1$ $\mu$s using a home built current regulation circuit (700 V, 50 A). Although smaller coils would offer the advantage of lower inductivity and thus a faster risetime for the field, a lower limit for the coil size is given by the requirement of avoiding collisions within the unskimmed molecular beam. Emission from the center of the molecular beam is selected by focusing through a 1 mm slit aperture and is detected by a photomultiplier tube (Hamamatsu R329-02). The resulting signal is sent to a digitizing oscilloscope (Le Croy 9450) and is stored on computer. The computer also gives the initial trigger for the pulsed valve and the excimer laser which is fired after a delay of about 200 $\mu$s. The recording of the molecular emission decay and the rise of the magnetic field are triggered by the UV laser beam which is detected by a second photomultiplier tube on a secondary reflection. This procedure diminishes jitter between the laser pulse and the rise of the field to $< 5$ ns. Three additional Helmholtz coils are placed around the vacuum chamber. They are used to compensate the earth magnetic field and to generate additional static fields. Table 1 summarizes details of the electronically excited states of $CS_2$ used in the present study.

## 3 Theoretical aspects

Following coherent excitation of magnetic sublevels split by an external magnetic field **B**, Zeeman quantum beats can be observed in the emission decay. Under the linear Zeeman regime where the energy separation between adjacent sublevels is $\Delta E = g_J \mu_B B$, $g_J$ and $\mu_B$ being the Landé factor for the state involved and the Bohr magneton respectively, the quantum beats occur at the Larmor frequency $\omega_L = g_J \mu_B B/\hbar$ and/or at $2\omega_L$ depending on the selection rules ($\Delta M = 1$ or $\Delta M = 2$) of the induced transitions [13]. In the case depicted in Figure 1 we start from the rovibronic ground state $|J_i = 0, M_i = 0\rangle$ of the $CS_2$ molecule and pump *via* an $R(0)$ optical transition a rovibronic state $|J = 1\rangle$ in an electronically excited state. Using $\sigma$ laser polarization ($\epsilon^L \perp \mathbf{B}$) the selection rule

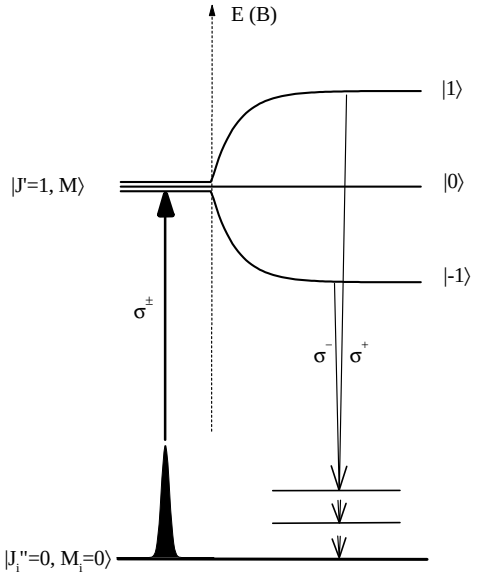


**Fig. 1.** Energy level diagram for excitation and emission of the $CS_2$ molecule before and after switching of the pulsed magnetic field, illustrated for a $R(0)$ transition.

$\Delta M = \pm 1$ allows the preparation of a superposition of the two states $|J = 1, M = +1\rangle$ and $|J = 1, M = -1\rangle$ thus creating $\Delta M = 2$ coherences. With $\pi$ polarized laser pulses ($\epsilon^L \parallel \mathbf{B}$) the system is excited to $|J = 1, M = 0\rangle$ and no quantum beats are observed. When the laser polarization is chosen between these two extremes, *i.e.* at an angle $\alpha$ relative to **B** with $0 < \alpha < 90°$, coherences among all the three sublevels are produced giving rise to $\Delta M = 1$ and $\Delta M = 2$ Zeeman quantum beats. The same selection rules apply to the polarization of the emission of the molecule. Polarized detection can be of advantage by enhancing the modulation depths of beats simply because the unmodulated emission is not polarized, or by enhancing sensitivity to $\Delta M = 1$ or $\Delta M = 2$ coherences (see below).

The response of the quantum system described above to a time dependent magnetic field will be treated by the density matrix formalism. Following *e.g.* Corney [21] and Blum [22], we note that the time dependence of the density operator $\rho$ is given by the Liouville equation

$$\frac{\partial \rho}{\partial t} = \frac{1}{i\hbar}[\mathbf{H}, \rho], \tag{1}$$

where **H** involves the unperturbed Hamiltonian and the Zeeman operator

$$\mathbf{H} = \mathbf{H}_0 + g_J \mu_B \mathbf{J} \cdot \mathbf{B}. \tag{2}$$

For a static magnetic field in $Z$ direction, we obtain

$$\frac{\partial \rho_{MM'}}{\partial t} = (-i\omega_L(M - M') - \Gamma)\rho_{MM'}, \tag{3}$$

where the relaxation of the system is introduced by the natural linewidth $\Gamma$, assumed to be the same for all sublevels. For the example in Figure 1, the elements of

the excited state density matrix have the simple form $\rho_{MM'} = \langle J = 1, M|\rho|J = 1, M'\rangle$. After integration of equation (3) we find

$$\rho_{MM'} \sim \sum_i F_{MM'}\rho_{ii} \exp\left[(-\Gamma - i\omega_L(M - M'))t\right]. \quad (4)$$

Here $\rho_{ii} = \langle J_i = 0, M_i = 0|\rho|J_i = 0, M_i = 0\rangle$ is the density matrix of the initial states $|i\rangle$ in the present case. The excitation process is described by the matrix

$$F_{MM'} = \langle M|\mathbf{e}_a \cdot \mathbf{D}|i\rangle\langle i|\mathbf{e}_a^* \cdot \mathbf{D}|M'\rangle \quad (5)$$

with $\mathbf{D}$ being the electric dipole transition moment operator and $\mathbf{e}_a$ the excitation polarization vector. The exponential term is related to the free evolution of the excited state matrix under the influence of the magnetic field and of the decay of the excited sublevels. The fluorescence intensity can be expressed by

$$I_f \sim \mathrm{Tr}(\rho L_f), \quad (6)$$

where $L_f$ represents the fluorescence monitoring operator given in this case by the detection matrix $G_{MM'}$. Using equation (4) we thus obtain

$$I_f \sim \sum_{M,M',i,f} F_{MM'}G_{M'M}\rho_{ii} \times \exp(-\Gamma t) \exp\left[-i\omega_L(M - M')t\right], \quad (7)$$

with the detection matrix

$$G_{M'M} = \langle M'|\mathbf{e}_d \cdot \mathbf{D}|f\rangle\langle f|\mathbf{e}_d^* \cdot \mathbf{D}|M\rangle \quad (8)$$

describing the emission towards the final states $|f\rangle$.

In the case of a time dependent magnetic field $\mathbf{B}(t)$, which is taken to be directed along a fixed direction defining the quantization axis, equation (3) becomes

$$\frac{\partial\rho_{MM'}}{\partial t} = \Big(-i\frac{g_J\mu_B}{\hbar}B(t)(M - M') - \Gamma\Big)\rho_{MM'}, \quad (9)$$

and integration of this expression yields

$$\rho_{MM'} \sim \sum_i F_{MM'}\rho_{ii} \exp(-\Gamma t) \times \exp\Big(-i(M - M')\frac{g_J\mu_B}{\hbar}\int_0^t B(t)dt\Big). \quad (10)$$

The second exponential function of equation (10) describes the explicit dependence of the excited state density matrix on the magnetic field. By applying equation (6), we finally obtain the fluorescence intensity as

$$I_f \sim \sum_{M,M',i,f} F_{MM'}G_{M'M}\rho_{ii} \exp(-\Gamma t) \times \exp\Big(-i(M - M')\frac{g_J\mu_B}{\hbar}\int_0^t B(t)dt\Big). \quad (11)$$

The functional form of the switched magnetic field used in the present study is discussed below in conjunction with the simulation of the experiment.

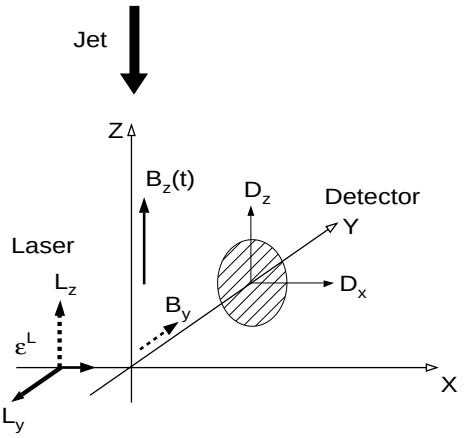


**Fig. 2.** Geometry of the experimental setup. The laser propagation, detection, and pulsed field $B_Z(t)$ directions define the $X$, $Y$ and $Z$ axes, respectively. For selected experiments polarized detection is used and an addition static magnetic field $B_Y$ is introduced.

## 4 Results

### 4.1 Creation and destruction of quantum beats

The geometry used in these experiments is shown in Figure 2. The switched magnetic field $B_Z(t)$ is oriented along the $Z$ axis which is chosen as the quantization axis. The laser beam propagates in $X$ direction, and is horizontally polarized $L_Y$ ($\sigma^{\pm}$ excitation), while the emission is detected in the $Y$ direction. Polarized detection may be achieved using a sheet polarizer if required. In the upper trace of Figure 3 we show the results obtained for the 17U $R(0)$ transition at 30 070.305 cm$^{-1}$. The jet-cooled molecules are initially excited under zero field conditions by a 3 ns laser pulse to the magnetically degenerate rotational state $|J = 1, M = \pm 1\rangle$ which subsequently gives rise to a simple exponential decay $\exp(-\Gamma t)$. After a given delay time, which in the present example was $\Delta t = 1.3$ $\mu$s, the magnetic field is suddenly switched on, splitting the three sublevels (see Fig. 1) and creating a pronounced quantum beat, superimposed on the exponential decay. This effect is described by the off-diagonal elements of the excited state density matrix, equation (10), where the expression $2g_J\mu_B/\hbar\int_0^t B(t)dt$ represents the phase difference $\Delta\varphi$ between the time evolution of the two sublevels $|J = 1, M = 1\rangle$ and $|J = 1, M = -1\rangle$. After the "$\delta$-pulse" excitation of the degenerate sublevels but before the onset of the magnetic field, $\Delta\varphi$ remains zero. Following the onset of the field $\Delta\varphi$ grows with $B$ as manifested by the appearance of a quantum beat with increasing beat frequency. After about a microsecond, the magnetic field has reached its stationary value $B_\infty \approx 100$ G and the quantum beat assumes a fixed frequency $2\omega_L = d(\Delta\varphi)/dt = 2g_J\mu_B B_\infty/\hbar$ which in the present case is $\approx 6.2$ MHz. For the chosen geometry and laser excitation *via* a $R(0)$ transition, the onset of $B$ is accompanied by an increase of the emission intensity relative to that for $B = 0$ ($\Delta\varphi = 0$).

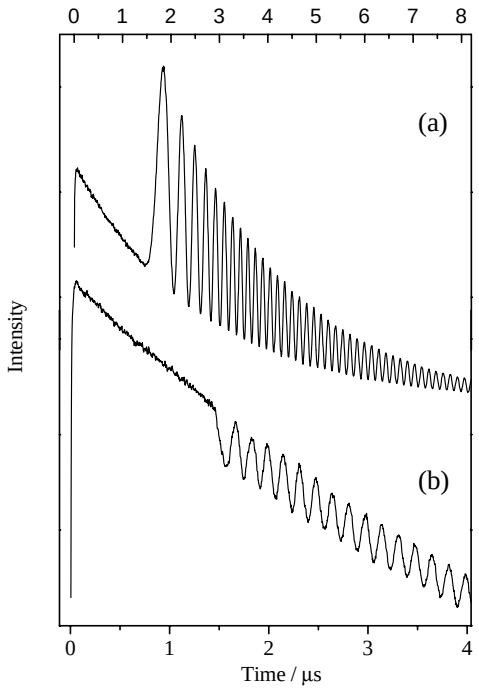


**Fig. 3.** Creation of coherences: fluorescence decays of $CS_2$ following excitation by a 3 ns pulse *via* the 17U $R(0)$ transition at 30 070.305 $cm^{-1}$ (upper trace) and 6V $Q(2)$ transition at 30 529.198 $cm^{-1}$ (lower trace). After a delay of 1.3 $\mu$s relative to the laser pulse, the magnetic field $B_Z(t)$ is switched on, creating the "up" and "down" modulated Zeeman quantum beats respectively.

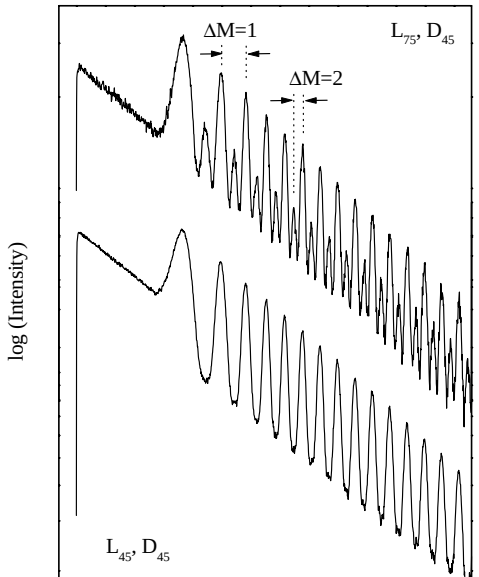


**Fig. 4.** Fluorescence decays of $CS_2$ using the 17U $R(0)$ excitation at 30 070.305 $cm^{-1}$ and polarized $D_{45}$ detection. After a delay of 1.25 $\mu$s $B_Z(t)$ is switched on producing $\Delta M = 1$ and $\Delta M = 2$ Zeeman quantum beats. The upper trace was taken with a laser polarization of $\alpha = 75°$, the lower trace with $\alpha = 45°$.

A decrease of emission intensity on switching the magnetic field may also be obtained, if for example laser excitation *via* the 6V $Q(2)$ transition at 30 529.198 $cm^{-1}$ (see Tab. 1) is applied. Under these conditions the magnetic field induces a quantum beat which reduces the emission intensity relative to that of the initially unmodulated decay as demonstrated in the lower trace of Figure 3 ($B_\infty \approx 10$ G). While for $R(0)$ excitation the coherent emission is initially predominantly directed at right angles relative to the detector, $Q(2)$ excitation leads to a favoured emission direction which coincides with the detector axis (see Fig. 2). It is noted, however, that the $Q(2)$ case is complicated by the contribution of three rotational transitions to the coherent emission: $P(3)$, $Q(2)$ and $R(1)$ respectively. Since the $P(3)$ and $Q(2)$ beats almost cancel because of their comparable amplitudes but opposite phases, the $R(1)$ transition, having the greatest modulation depth and an initial phase corresponding to a maximum intensity, determines the form of the observed quantum beat (see simulations below).

Finally by changing the angle $\alpha$ between the laser polarization and magnetic field from a perpendicular geometry, $\Delta M = 1$ coherences may be prepared in addition to the $\Delta M = 2$ coherences observed in the above measurements. The amplitudes of the two sets of coherences have different dependences on $\alpha$ allowing the fraction of each present to be varied. In Figure 4 we illustrate the effect of varying $\alpha$ with a fixed $D_{45}$ detection geometry for the $R(0)$ transition. The upper trace shows the decay recorded with $\alpha = 75°$. On switching the magnetic field 1.25 $\mu$s after the laser pulse, $\Delta M = 1$ and $\Delta M = 2$ coherences are observed with similar strengths. In the lower trace, recorded with $\alpha = 45°$ excitation, the $\Delta M = 2$ coherences are now substantially weaker and are only discernable by the asymmetric shape of the $\Delta M = 1$ beats. We note also that for this geometry the beat intensity oscillates above and below the zero field intensity (compare also Fig. 3).

Our next results are concerned with the controlled elimination of quantum beats. Although our pulsed magnetic field has a risetime of 0.3 $\mu$s, the fall-off time which is determined by the time to remove the stored energy in the coil is much larger (several hundreds of microseconds). However, a rapid quenching of the magnetic field can be realized by applying a static magnetic field and nulling it with a switched field of equal magnitude in the opposite direction. The field can thus be "switched off" in a controlled manner; in the present case at a particular phase of the quantum beats. In the examples shown in Figure 5, the 17U $R(0)$ transition was excited in the presence of a static field of 16 Gauss producing a coherence between the $|M = +1\rangle$ and $|M = -1\rangle$ states which leads to quantum beats of 1 MHz on the molecular emission decays. After $t = 4$ $\mu$s (upper trace) and 3.35 $\mu$s (lower trace) relative to the laser pulse, the magnetic field was switched off "freezing" the superposition state $|J = 1, M = \pm 1\rangle$ at the maximum (upper trace) or the minimum (lower trace) of the beat amplitude. The subsequent emission intensity is unmodulated but still shows the characteristic angular

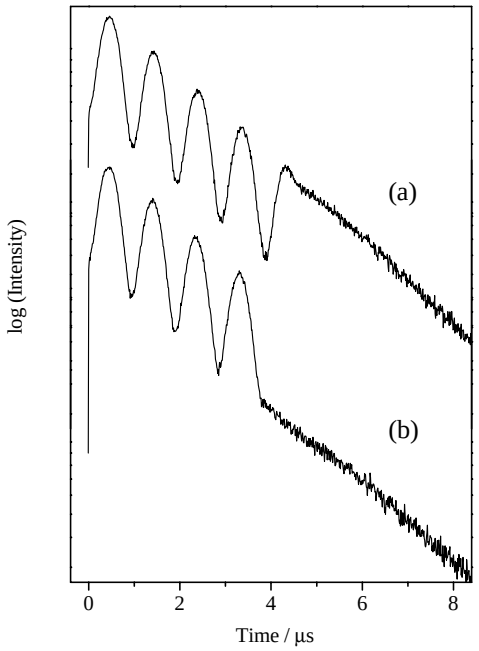


**Fig. 5.** Destruction of coherences. The magnetic field is nulled after a delay of 4 $\mu$s (upper trace) and 3.35 $\mu$s (lower trace), thus "freezing" the relative phases of the superposition state. Excitation was into the 17U $R(0)$ transition of $CS_2$ and the initial static field was 16 Gauss.

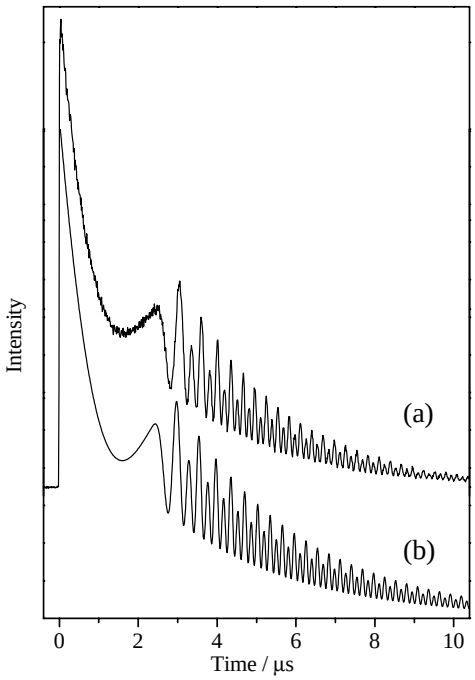


**Fig. 6.** Effect on coherences of switching the quantization axis using a combination of a static and a pulsed magnetic field. Following excitation of $CS_2$ 17U $R(0)$ under a weak static field of $B_Y = 3$ G, the stronger field $B_Z(t)$ is switched after 2.25 $\mu$s. $D_{45}$ detection uncovers the slow beat under $B_Y$ and the $\Delta M = 1$ and $\Delta M = 2$ coherences generated by the pulsed field (upper trace). The lower trace shows the numerical simulation.

distribution of the coherent superposition states prior to the annihilation of the field. Thus by choosing the phase of the superposition state at which **B** is switched off, we select the intensity of the subsequent emission.

Our molecular beam experiment, which provides isolated molecule conditions, further indicates that the fast rise of the switched field has no perturbing effect on the phase of the created Zeeman quantum beats. The beat amplitudes decay without detectable dephasing, in other words they decay according to the decay constant of the initially unmodulated decay as demonstrated by the logarithmic plots shown in Figure 4. This result justifies our assumption that the off-diagonal and diagonal elements of the density matrix equation (10) are damped with the same decay constant. However switching a magnetic field which is *inhomogeneous* over the sample volume was shown to produce an ensemble of molecules with different beat frequencies. After the field onset, the thus created beats interfere destructively which is manifested by an apparent dephasing.

### 4.2 Probing of coherences by switching the quantization axes

The versatility of the above experiments can be extended by the introduction of a second magnetic field. We present here an example where a transient magnetic field $B_Z(t)$ probes the temporal evolution of coherences which have been generated with a weak static magnetic field $B_Y$. Since $B_Z(t)$ is chosen to be orthogonal to $B_Y$, it switches the quantization axis of the system thus modifying the emission properties of the initial superposition state. For these experiments, the setup shown in Figure 2 was modified as follows. The laser, still directed along the $X$ axis, now has $L_Z$ polarization and a static magnetic field along the $Y$ axis has been added which defines the initial quantization axis. After a time delay $\Delta t$ following the laser pulse excitation, the pulsed field is switched along the $Z$ axis and rotates the initial quantization axis. Detection remains along the $Y$ direction.

For these experiments, the 17U $R(0)$ transition of $CS_2$ at 30 070.305 $cm^{-1}$ (see Tab. 1) was investigated and the essentially $\delta$-pulse laser excitation prepared a superposition of the $|M_Y = +1\rangle$ and $|M_Y = -1\rangle$ levels which are split in energy by the static field $B_Y$. After a variable evolution $\Delta t$, the much stronger pulsed magnetic field $B_Z(t)$ was switched on, rotating the quantization axis into the $Z$ direction. (We note that the contribution of the $B_Y \approx 2$ G field is negligible as $B_Z(\infty) \approx 100$ G.) The upper trace in Figure 6 shows the resulting emission recorded with a delay $\Delta t$ =2.25 $\mu$s, illustrating that the "axis switching" is manifested by the appearance of distinct higher frequency quantum beats. The example displayed here was recorded using $D_{45}$ detection in order to illustrate both $\Delta M = 1$ and $\Delta M = 2$ coherences as well as the slow modulation of the initially prepared superposition state $|M_Y = \pm 1\rangle$, the evolution of which is stopped when the pulsed field is switched on. The projection of the $|M_Y = \pm 1\rangle$ levels onto

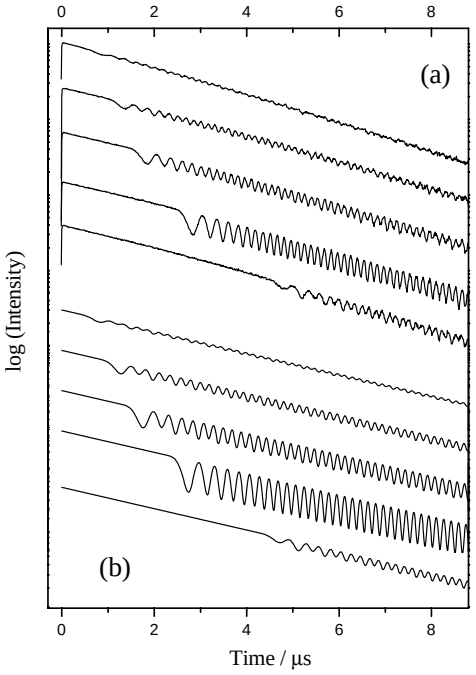


**Fig. 7.** Probing the initial coherence. Measured data (a) and numerical simulations (b) of the crossed magnetic field experiment (see Fig. 6) but with delays (0.25, 0.75, 1.25, 2.25 and 4.25 $\mu$s) for $B_Z(t)$ and unpolarized detection.

a basis determined by the pulsed magnetic field results in a coherent superposition of the $|M_Z = +1\rangle$, $|M_Z = 0\rangle$ and $|M_Z = -1\rangle$ states. Figure 7a shows the appearance of the emission after various delays between the laser excitation and the pulsed field recorded using unpolarized detection. The modulation of the $|M_Y = \pm 1\rangle$ superposition is now not observable, however the magnitude of the pulsed field-induced quantum beats depends on the delay $\Delta t$ and indeed reflects the phase difference between the initially coherently prepared $|M_Y = +1\rangle$ and $|M_Y = -1\rangle$ states. The presence of the $\Delta M = 1$ beats in addition to the $\Delta M = 2$ beats is a consequence of the slightly non-orthogonal geometry due to the weak $B_Y$ field. In contrast to the measurements displayed in Figure 7, the decay in Figure 6a was recorded with polarized detection which gives rise to an enhanced modulation depth for the $\Delta M = 1$ beats.

### 4.3 Simulation

To examine our experimental results and to reveal details of the decay characteristics, we carried out some numerical simulations. This was achieved by obtaining the derivative of the density matrix using the Liouville equation, followed by subsequent integration This general procedure allows us to simulate not only the data obtained with the switched field but also those with the additional static field. The axis system was chosen according to Figure 2 and the excitation/detection polarizations are referenced to this. The magnetic field is treated in terms of its Cartesian components and we rewrite the Zeeman term in equation (2) as

$$H_Z = g_J \mu_B (B_X J_X + B_Y J_Y + B_Z J_Z). \quad (12)$$

For the purpose of the simulations, the switched field $B_Z(t)$ was assumed (in close agreement with the experiment) to have the form

$$B_Z(t) = B_\infty (1 - \exp[-(t - t_{on})/\tau]), \quad (13)$$

where $\tau$ is the risetime of the field. As the operators $J_X$ and $J_Y$ have non-diagonal matrix elements yielding cross terms in the derivative of the density matrix, numerical integration of the Liouville equation becomes necessary. The excitation matrix $F_{MM'}$ (Eq. (5)) may be expressed as [21,23]

$$F_{MM'} = \sum_{M_i} (-1)^{2J-M-M'+q} \begin{pmatrix} J & 1 & J_i \\ -M & q & M_i \end{pmatrix} \times \begin{pmatrix} J & 1 & J_i \\ -M' & q' & M_i \end{pmatrix} \mathbf{e}_{-q} \cdot \mathbf{e}_{q'} |\langle J||\mathbf{D}||J_i\rangle|^2. \quad (14)$$

The polarization components of $\mathbf{e}_q$ are given by

$$\mathbf{e}_{\pm 1} = -i \sin\alpha/\sqrt{2},\ \mathbf{e}_0 = -\cos\alpha, \quad (15)$$

where $\alpha$ is the angle for the polarization with respect to the $Z$ axis. The detection matrix (Eq. (8)) is obtained analogously but is summed over all possible final rotational states [21,22]

$$G_{MM'} = \sum_{J_f M_f} (-1)^{2J-M-M'+r'} \begin{pmatrix} J & 1 & J_f \\ -M' & r' & M_f \end{pmatrix} \times \begin{pmatrix} J & 1 & J_f \\ -M & r & M_f \end{pmatrix} \mathbf{e}_{-r'} \cdot \mathbf{e}_r |\langle J||\mathbf{D}||J_f\rangle|^2 \quad (16)$$

where

$$\mathbf{e}_{\pm 1} = \pm \sin\alpha/\sqrt{2},\ \mathbf{e}_0 = -\cos\alpha. \quad (17)$$

In the simulations we calculate the individual contribution of each detection channel by approximating the reduced matrix elements $|\langle J||\mathbf{D}||J_f\rangle|^2$ to the Hönl-London factors [23]

$$|\langle J||\mathbf{D}||J_f\rangle|^2 = (2J+1)(2J_f+1) \begin{pmatrix} J_f & 1 & J \\ -K & 0 & K \end{pmatrix}^2. \quad (18)$$

We first simulated the results obtained solely with the switched field. Simulation of the 17U $R(0)$ transition (experimental result given in the upper trace of Fig. 3) showed good agreement with experiment and illustrated that the $R(0)/R(0)$ excitation/detection scheme leads to a 100% beat modulation; the incoherent contributions observed on the experimental decay arise exclusively from the superimposed $P(2)$ detection step. Figure 8 shows the

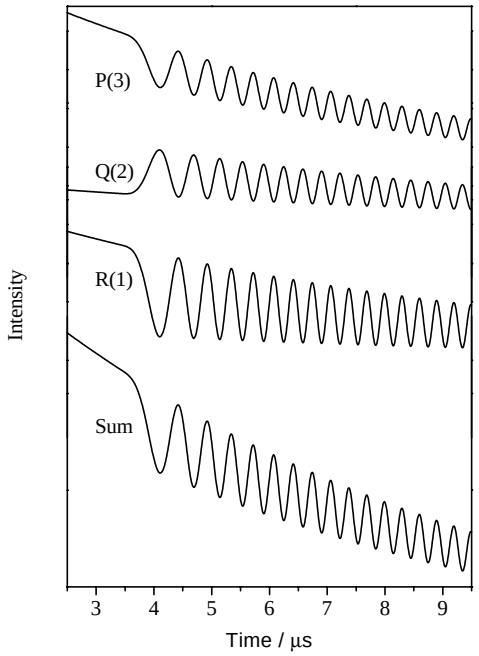


**Fig. 8.** Results of the simulation for the 6V $Q(2)$ transition, the experimental decay for which is shown in Figure 3, illustrating the contributions of the $P(3)$, $Q(2)$ and $R(1)$ detection channels to the total emission.

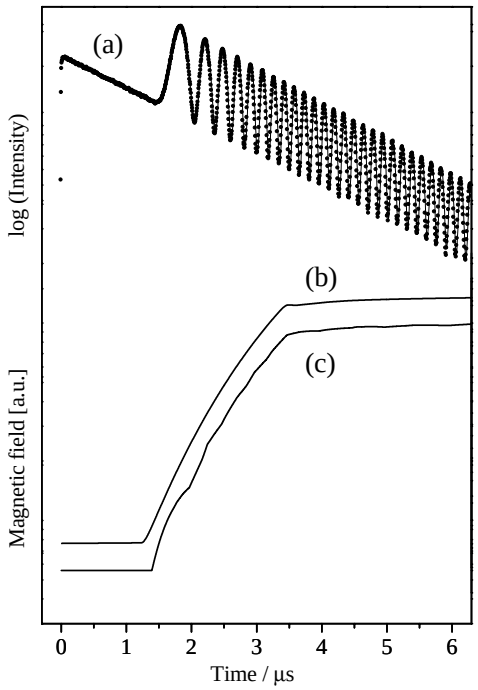


**Fig. 9.** Temporal behavior of the magnetic field $B_Z(t)$. The experimental data is shown by the dots in the decay (a) while the line represents the results of the fitting procedure which provided the $B_Z(t)$ curve (c). Trace (b) gives the result of the measurement from a small induction coil.

result of the simulation for the 6V $Q(2)$ transition displayed in the lower trace of Figure 3 and reveals the contributions from three rotational detection transitions. It can be seen that the quantum beat on the $Q(2)$ channels is of opposite phase to that for the $R(1)$ and $P(3)$ transitions. Furthermore as discussed above, the $Q$ and $P$ contributions effectively cancel leaving the $R(1)$ detection channel to determine the form of the quantum beat.

The good agreement between the simulations and the experiments led us to extract the exact temporal behavior of the magnetic field $B(t)$. We used the results obtained for the 17U $R(0)$ transition and assumed the magnetic field to have the initial form given in equation (13). The beating term for the decay was calculated and was then multiplied with a suitable exponential decay to allow exact agreement with the experimental lifetime and modulation depth. The form of $B_Z(t)$ was then altered until satisfactory agreement with the experimental results was achieved. The results are shown in Figure 9, where the decay (a) clearly shows the agreement between simulation and experiment. The form of $B_Z$ obtained is shown in trace (c). In an independent measurement of the magnetic field, a small induction coil was placed between the Helmholtz coils, yielding trace (b). The excellent agreement between the direct field measurements and $B_Z(t)$ extracted from the beat dynamics also justifies our assumption of an adiabatic description for the creation of the coherences.

Before presenting the results of the simulations for the case of the combined magnetic fields, we briefly discuss in an analytical manner the effect of projecting the prepared coherence onto a different axis system. Under the initial $Y$ axis quantization, the initial superposition state is described by

$$\rho^Y = \frac{1}{2}\begin{pmatrix} 1 & 0 & \exp(i\varphi) \\ 0 & 0 & 0 \\ \exp(-i\varphi) & 0 & 1 \end{pmatrix}, \qquad (19)$$

where the diagonal elements give the population of the substrates in the order $M_Y = -1,\ 0,\ 1$. The exponential factors $\exp(\pm i\varphi)$ allows for a phase difference between the levels which has been acquired during the evolution in the static magnetic field. Projection of this matrix onto $Z$ axis quantization yields

$$\rho^Z = \frac{1}{4}\begin{pmatrix} 1+\cos\varphi & \sqrt{2}i\,\sin\varphi & 1+\cos\varphi \\ -\sqrt{2}i\,\sin\varphi & 2(1-\cos\varphi) & -\sqrt{2}i\,\sin\varphi \\ 1+\cos\varphi & \sqrt{2}i\,\sin\varphi & 1+\cos\varphi \end{pmatrix}. \qquad (20)$$

This shows that the population of the $Z$ axis sublevels and the coherence between them is dependent on the phase difference $\varphi$ acquired before projection. Depending on the delay, population oscillates between the $|M_Z = \pm 1\rangle$ levels and the $|M_Z = 0\rangle$ level, as does the strength of the $\Delta M = 1$ and $\Delta M = 2$ coherences.

The lower trace (b) in Figure 6 gives the result of the numerical simulation for the $D_{45}$ detection combined field experiment which shows excellent agreement with experiment. The simulations of the variable delay measurements are shown in Figure 7. The unpolarized detection was simulated by calculating the decays for both $D_0$ and $D_{90}$

detection and then taking the sum. Analysis of the two polarizations illustrates the effect of the switched field on the molecular coherence and its emission. The initial coherence is, as noted above, not observable using unpolarized detection as the beat emission for the two orthogonal polarizations is of opposite phase. However following rotation of the quantization axis on switching on the pulsed field, the vertical detection polarization carries the majority of the quantum beat emission. The horizontal polarization is only very weakly modulated at the frequency of the $\Delta M = 1$ beat. As discussed above, this is a consequence of the slight non-orthogonality of the switched quantization axes.

## 5 Discussion and conclusions

In this work we have applied a series of experiments to study the interaction of a rapidly switched magnetic field on electronically excited levels in $CS_2$. These are accessed using a short Fourier-transform-limited laser pulse with a duration (3 ns) more than two orders of magnitude shorter than the other timescales involved in the experiment and a bandwidth substantially greater than any of the splittings between the excited levels. Thus excitation may be regarded essentially as that from a $\delta$-pulse, ensuring that the excited states are prepared with a well-defined relative phase. The evolution of the resulting coherences is investigated by observing the fluorescence emission of the sample with polarized detection being used to enhance sensitivity to specific coherences when required. Two main classes of experiments were carried out. In the first set, the pulsed field was used to investigate the creation and destruction of molecular coherences while in the second the effect of a rotation of quantization axis on molecular coherences was investigated.

In the coherence creation experiment, the setup of which has similarities to that used to investigate the Hanle effect [2,23–25], the magnetic field was switched on after the field-free laser excitation. Dependent on the experimental geometry, $\Delta M = 2$ and $\Delta M = 1$, only $\Delta M = 2$, or no coherences were created. The "freezing" of these coherences into a superposition state with a fixed phase was demonstrated with the coherence destruction experiments. The results showed that the rate constants for the decay of quantum beat modulation and incoherent (exponential) decay are identical and that the quantum beat modulation depth is identical when either a static or pulsed magnetic field is used. This was also found to be the case, independent of the delay between the field and the laser. This observation leads us to conclude firstly that the pulsed field is homogeneous over the interaction region (no dephasing is observed) and secondly that the interaction of the molecule with the pulsed field is adiabatic on the time scale of the field risetime. As a consequence, the induced quantum beat can be exploited to characterize the temporal form of the pulsed field. Comparison of the field obtained in this manner with that measured with an induction coil showed excellent agreement. The quantum beat method of course yields an absolute measurement of the field.

The experiments with a combination of static and pulsed fields were then carried out to further investigate the response of molecular coherences to fast perturbations. Laser excitation initially produced a $\Delta M = 2$ coherence in one quantization axis which was then projected onto a new (nearly) perpendicular axis by switching on the pulsed field after a given delay. With unpolarized detection the fluorescence decay was measured to be exponential (*i.e.* unmodulated) until the pulsed field was switched on, when quantum beats are observed. Importantly the magnitude of the beat amplitudes was found to depend on the phase of the initially prepared coherence at the moment the field was switched on. In the matrix formulation discussed in the section above this behavior was predicted in that the populations of the final Zeeman states and the magnitudes of the resulting $\Delta M = 2$ and $\Delta M = 1$ coherences have a periodic dependence on this phase. In physical terms, the pulsed field converts the manifestation of the initially prepared coherence from that of a rotating polarization vector (which is not detectable to unpolarized detection) before switching the field to an oscillation in the fluorescence intensity (quantum beat) after switching. The use of polarized detection allowed us to observe the evolution of the coherences before and after the switching of the magnetic field and showed that the modulation depth of the quantum beat of the induced beat is not attenuated by the "axis switching", which adds further evidence for the adiabatic nature of the interaction of molecule and field on this time scale. Furthermore our experiments demonstrated that appropriate nulling of the fields can provide a method for preparation of molecules in a more general superposition state, characterized by coherences among all participating sublevels.

In considering possible future work in this area, a priority is certainly to study the effect of faster perturbations on molecular coherences. Although our results indicate that the interaction of the molecule with the pulsed field is adiabatic over the sub-microsecond risetime of the field, it would be interesting to investigate this on a shorter time scale. The present work has focused on the use of a pulsed magnetic field, however rapidly switched electric fields might also be applied *i.e.* the Stark equivalent to the present Zeeman studies. Pulsed electric fields have been previously used by Brewer and others but, in contrast to the present work, with c.w. excitation, allowing effects such as optical nutation, photon echoes and Raman beats to be studied [26].

Support of this work by the Schweizerischer Nationalfonds is gratefully acknowledged. We thank Hermann Schwarz for his help in developing the pulsed field apparatus, and Dr H. Nagai for preliminary experiments.

## References


1. S. Haroche, in *High Resolution Laser Spectroscopy*, edited by K. Shimoda (Springer, Berlin, 1976).
2. E.B. Alexandrov, M.P. Chaika, G.I Khvostenko, *Interference of Atomic States* (Springer, Berlin, 1993).
3. H. Bitto, J.R. Huber, in *Nonlinear Spectroscopy for Molecular Structure Determination*, edited by R.W. Field, E. Hirota, J.P. Maier, S. Tsuchiya (Blackwell Science, Oxford, 1998).
4. E. Hack, J.R. Huber, Int. Rev. Phys. Chem. **10**, 287 (1991).
5. H. Bitto, J.R. Huber, Opt. Commun. **80**, 184 (1990).
6. R.T. Carter, K.F. Schmidt, H. Bitto, J.R. Huber, Chem. Phys. Lett. **257**, 297 (1996).
7. R.T. Carter, I.M. Povey, H. Bitto, J.R. Huber, J. Chem. Phys. **104**, 5365 (1996).
8. Th. Walther, H. Bitto, T.K. Minton, J.R. Huber, Chem. Phys. Lett. **231**, 64 (1994).
9. R.T. Carter, Th. Walther, H. Bitto, J.R. Huber, Chem. Phys. Lett. **240**, 79 (1995).
10. K. Bergmann, H. Theuer, B.W. Shore, Rev. Mod. Phys., and references therein (in press).
11. P. Brumer, M. Shapiro, Phil. Trans. R. Soc. Lond. A **355**, 2409 (1997) and references therein.
12. P. Brumer, M. Shapiro, Chem. Phys. **217**, 325 (1997).
13. H. Bitto, A. Levinger, J.R. Huber, Z. Phys. D **28**, 303 (1993).
14. A. Levinger, H. Bitto, J.R. Huber, Opt. Commun. **103**, 381 (1993).
15. D.T. Cramb, H. Bitto, J.R. Huber, J. Chem. Phys. **96**, 8761 (1992).
16. H. Bitto, A. Ruzicic, J.R. Huber, Chem. Phys. **189**, 713 (1994).
17. B. Kleman, Can. J. Phys. **41**, 2034 (1963).
18. C. Jungen, D.N. Malm, A.J. Merer, Can. J. Phys. **51**, 1471 (1973).
19. K. Nishizawa, S. Kubo, A. Doi, H. Katô, J. Chem. Phys. **100**, 3394 (1994).
20. A. Habib, R. Lange, G. Brasen, W. Demtröder, Ber. Bunsenges. Phys. Chem. **99**, 265 (1995).
21. A. Corney, *Atomic and Laser Spectroscopy* (Clarendon Press, Oxford, 1977).
22. K. Blum, *Density Matrix Theory and Applications* (Plenum Press, New York, 1981).
23. R.N. Zare, *Angular Momentum* (Wiley, New York, 1988).
24. W. Hanle, Z. Phys. **30**, 93 (1924).
25. R.N. Zare, Acc. Chem. Res. **4**, 361 (1971).
26. R.G. Brewer, in *Very High Resolution Spectroscopy*, edited by R.A. Smith (Academic Press, London, 1976) and references therein.